

Aspects of the phase diagram in (P)NJL-like models

M. Buballa,¹ A.G. Grunfeld,^{2,3} A.E. Radzhabov,⁴ D. Scheffler¹

¹Institut für Kernphysik, Technische Universität Darmstadt, Germany

²CONICET, Buenos Aires, Argentina

³Physics Dept., Comisión Nacional de Energía Atómica, Buenos Aires, Argentina

⁴Institute for System Dynamics and Control Theory, Irkutsk, Russia

August 13, 2018

Abstract

We discuss three applications of NJL- and PNJL-like models to assess aspects of the QCD phase diagram: First, we study the effect of mesonic correlations on the pressure below and above the finite temperature phase transition within a nonlocal PNJL model beyond the mean-field approximation. Second, we reconstruct the phase boundary of an NJL model from a Taylor expansion of the chiral susceptibility about $\mu = 0$ and compare the result with the exact phase boundary. Finally, we demonstrate the realization of the “non-standard scenario” for the critical surface in a three-flavor PNJL model with a μ -dependent determinant interaction.

1 Introduction

The investigation of the QCD phase transition and the structure of the phase diagram is certainly one of the most exciting areas in the field of strong interaction physics. A theoretical approach to these questions requires non-perturbative methods, which also provide a proper understanding of the chiral quark dynamics and the confinement mechanism. Until now, the only method which is directly based on QCD and which meets these requirements is lattice gauge theory. Unfortunately, the application of lattice results to experimental data is complicated by the fact that most lattice calculations are often performed with rather large quark masses, leading to unphysically large pion masses. Even more difficult is the extension of lattice calculations to nonvanishing chemical potentials, where the standard importance sampling techniques are spoiled by the “sign problem”. To bridge this gap between existing lattice data and phenomenologically interesting regimes which are not yet accessible by first principles, effective models which share the relevant symmetries with QCD can deal as useful tools. In this context, the Nambu–Jona-Lasinio (NJL) model is probably the most popular example. More recently, the Polyakov-loop extended Nambu–Jona-Lasinio (PNJL) [1, 2] has received increasing interest, as it allows to investigate both, the chiral and the deconfinement phase transition by studying the corresponding order parameters. Moreover, the coupling of the quark dynamics to the Polyakov loop cures, at least to a large extent, one of the most disturbing features of the NJL model, namely the contribution of unconfined quarks to the pressure at low temperatures and densities.

In the following, we will discuss three applications of NJL and PNJL-models to issues related to the phase diagram.

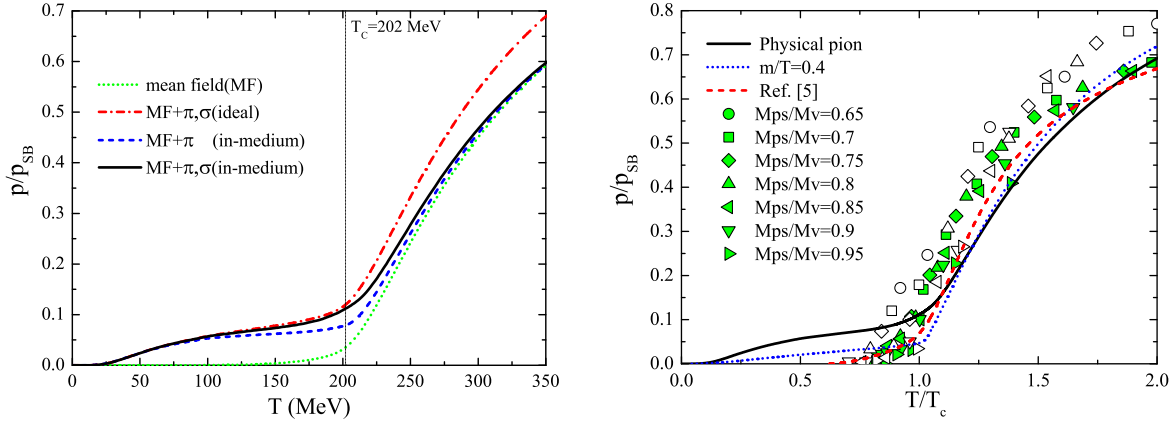


Figure 1: Left: Scaled pressure p/p_{SB} in the nonlocal PNJL model with the physical pion mass: mean field contribution (green dotted line), mean field + pion (blue dashed line), mean field + pion + sigma (black solid line). The red dash-dotted line denotes the scaled pressure of an ideal pion + sigma gas with fixed masses. Right: Scaled pressure p/p_{SB} as a function of T/T_c : non-local PNJL model with physical pion mass (black solid line) and with $m_c/T = 0.4$ (blue dotted line). Red dashed line: Lattice data for two-flavor QCD with staggered quarks [5]. Points: Lattice data for two-flavor QCD with Wilson-type quarks [6] for $N_t = 6$ (open symbols) and $N_t = 4$ (green filled symbols). The data for the pressure [6] have been divided by the Stefan-Boltzmann limit for $N_t = 6$ and $N_t = 4$, respectively, as given in Ref. [6]. Figures adapted from Ref. [4].

2 Effects of mesonic correlations

In spite of the simplicity of the PNJL model, a remarkable agreement with the results of lattice QCD thermodynamics have been obtained in Ref. [3]. However, that comparison was not entirely consistent: Whereas unphysically large values of the current quark masses have been used in the lattice simulations, physical values have been employed in the PNJL model analysis of Ref. [3]. Moreover, after successfully removing (most of) the unphysical quark degrees of freedom from the confined phase, the PNJL model treated in mean-field approximation as in Ref. [3] does not contain *any* degree of freedom in this regime. Obviously, this is a rather poor description of the hadronic phase at finite temperature where mesons are expected to become relevant. Hence, the good agreement of the PNJL results with the lattice data could be partially accidental in that mesonic correlations have been neglected in the PNJL analysis, while in the lattice calculations they are suppressed by the large current quark masses. To get a consistent picture one should thus go beyond the mean-field approximation and include mesonic correlations.

Here we briefly discuss the main results of Ref. [4], where we have done this in the framework of a $1/N_c$ expansion to next-to-leading order. Up to an additive constant, the thermodynamic potential at $\mu = 0$ is then given by $\Omega(T) = \Omega_{\text{mean field}}(T) + \Omega_{\text{corr}}(T)$ where the correlation part

$$\Omega_{\text{corr}}(T) = \sum_{M=\pi,\sigma} d_M \frac{T}{2} \sum_m \int \frac{d^3p}{(2\pi)^3} \ln [1 - G\Pi_M(\vec{p}, \omega_m)] \quad (1)$$

corresponds to the ring-sum of RPA-like polarization loops Π_M in the mesonic channel M with degeneracy factor d_M . These terms are worked out within a two-flavor PNJL-type model with a nonlocal 4-point interaction in the quark sector with a Gaussian form factor. This interaction has the advantage that all diagrams are finite. Further details of the model can be found in Ref. [4].

Our main results are shown in Fig. 1. On the left hand side, the pressure $p(T) = -\Omega(T)$, divided

by the Stefan-Boltzmann limit, is displayed as a function of the temperature. For comparison with the full result we also show the mean-field result and the mean-field plus pion contribution as well as the result for an ideal pion and sigma gas with the masses fixed at their vacuum values. We find that at low temperatures the mean-field (i.e., quark) contribution is suppressed and the pressure can be well described by a free pion gas. Near the critical temperature the σ meson gives an additional visible contribution whereas already for $T > 1.5 T_c$ the mesonic contributions are negligible and the quark-gluon mean-field dominates the pressure.

The results shown in the left panel of Fig. 1 have been obtained using realistic parameters with a current quark mass $m = 5.8$ MeV, corresponding to the physical pion mass of 140 MeV in vacuum. On the other hand, in most lattice calculations the masses are considerably larger. Thus in order to perform a meaningful comparison with lattice results, we should repeat our model calculations using quark masses similar to the lattice ones. To be specific, we choose the current quark mass to scale with the temperature as $m = 0.4 T$, mimicking the situation in the lattice calculation of Ref. [5], where the up and down quark masses behave in this way. The resulting pressure is displayed by the blue dotted line in the right panel of Fig. 1. For comparison we show again the result obtained with $m = 5.8$ MeV (black solid line). With $m = 0.4 T$ the qualitative behavior remains unchanged. Quantitatively, the meson contributions are of course suppressed by their higher masses, but they are still visible.

The red dashed line indicates the result of Ref. [5] obtained on a $16^3 \times 4$ lattice with improved staggered fermion actions for two flavors. As mentioned above, in this calculation the quark mass scales with the temperature, $m_{u,d}/T = 0.4$ and should therefore be compared with the blue dotted line. In the figure, we also show the lattice results of Ref. [6] for Wilson fermions. Although these data have been extracted for T -independent quark masses and are therefore not entirely comparable to the staggered fermion data (and to our calculations), they show a similar tendency.

Whereas in our model, even for $m = 0.4 T$, there remains a visible pion contribution to the pressure down to $T/T_c \approx 0.2$, the lattice pressure of [5] vanishes at $T/T_c = 0.6$. This discrepancy has a trivial explanation by the fact that the lattice pressure has been obtained by the “integral method” which leaves one integration constant undetermined. In Ref. [5], this constant has been fixed by the choice that the pressure vanishes at $T/T_c = 0.6$. On the other hand, chiral perturbation theory predicts that at very low temperature the pressure is well described by an ideal pion gas, in good agreement with our model. Hence, if the integration constant on the lattice had been fitted to χPT , rather than setting the pressure at $T = 0.6 T_c$ equal to zero, there would be good agreement with our results at this point. On the other hand, our approach underestimates the lattice data in the region between about 0.9 and 1.6 T_c . The missing pressure would be even larger if we shift the lattice pressure upwards to obtain agreement at $T = 0.6 T_c$. This indicates that hadronic resonances, other than pion and sigma become important in this regime and should be taken into account in improved versions of the model.

3 Assessing the phase diagram via Taylor expansion

As pointed out in the introduction a straight forward application of standard lattice techniques to the regime of non-vanishing quark number chemical potential μ is not possible. In this context various methods have been suggested to circumvent these problems. One of these methods consists in performing a Taylor expansion of the pressure in powers of μ/T , with the Taylor coefficients evaluated at $\mu = 0$,

$$\frac{p}{T^4}(T, \mu) = \sum_{n=0}^{\infty} c_n(T) \left(\frac{\mu}{T}\right)^n, \quad c_n(T) = \frac{1}{n!} \left. \frac{\partial}{\partial (\mu/T)^n} \left(\frac{p}{T^4}(T, \mu)\right) \right|_{\mu=0}. \quad (2)$$

One may also consider different chemical potentials for up, down, and strange quarks or, equivalently, for baryon number, electric charge and strangeness, but here we want to restrict ourselves to the case of a single chemical potential. Because of charge conjugation symmetry, only even powers in μ/T appear.

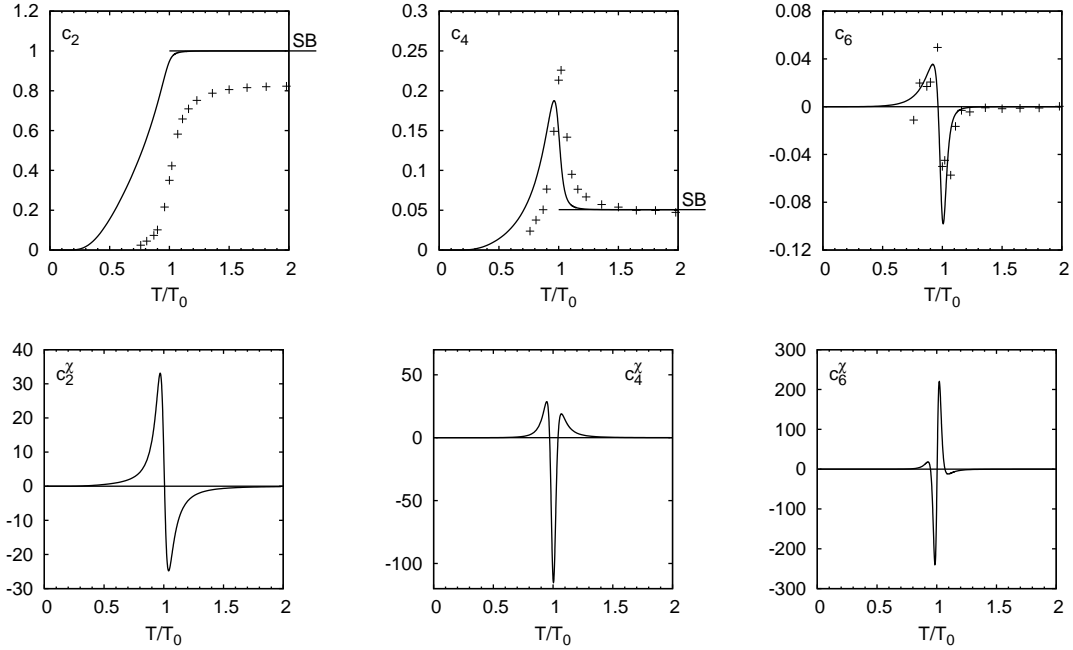


Figure 2: Taylor expansion coefficients c_n (upper panels) and c_n^x (lower panels) for $n = 2, 4, 6$ as functions of T/T_0 (lines). Also shown are lattice results for c_n from Ref. [8] (points). Adapted from Ref. [9].

In recent lattice calculations coefficients up to $n = 8$ have been calculated [7], but most studies so far were restricted to $n \leq 6$ [8]. It is then a natural question, how reliably this information can be used to reconstruct the phase boundary at non-zero μ . It would also be interesting to know whether one could find signatures of a critical endpoint in this way. Such questions can be addressed by performing a Taylor expansion in a model where the phase boundary and the location of the critical endpoint are known “exactly” (in the sense of the model).

Here we want to discuss some results of Ref. [9], where the Taylor expansion has been studied within a two-flavor NJL model without Polyakov loop in mean-field approximation. The “exact” phase diagram of that model is shown in the left panel of Fig. 3. At large chemical potentials we find a first-order phase boundary (solid line), which ends at a critical point at $\mu/T \approx 4$. For lower values of μ/T , there is a smooth crossover, which is indicated by the dotted line. This crossover line has been defined as the maxima of the reduced chiral susceptibility,

$$\frac{\chi_{mm}(T, \mu)}{T^2} = \frac{1}{T^2} \frac{\partial^2 p(T, \mu)}{\partial m^2}, \quad (3)$$

along lines of constant μ/T . Here m is the current quark mass parameter of the NJL model. Eq. (3) can be Taylor expanded as well. Employing Eq. (2) we obtain

$$\frac{\chi_{mm}(T, \mu)}{T^2} = \sum_{n=0}^{\infty} c_n^x(T) \left(\frac{\mu}{T}\right)^n, \quad c_n^x = T^2 \frac{\partial^2 c_n}{\partial m^2}. \quad (4)$$

In Fig. 2 the coefficients c_n and c_n^x for $n = 2, 4, 6$ are displayed as functions of T/T_0 , where T_0 is the crossover temperature at $\mu = 0$. Our model results are indicated by the lines. For the c_n we also show the lattice results of Ref. [8] for illustration. We see that the qualitative behavior is similar, but there are quantitative differences. In particular the Stefan Boltzmann limits, which are also indicated in the figure, are reached much faster in the model. This is an artifact of the NJL model which can be improved considerably by including the Polyakov loop [10].

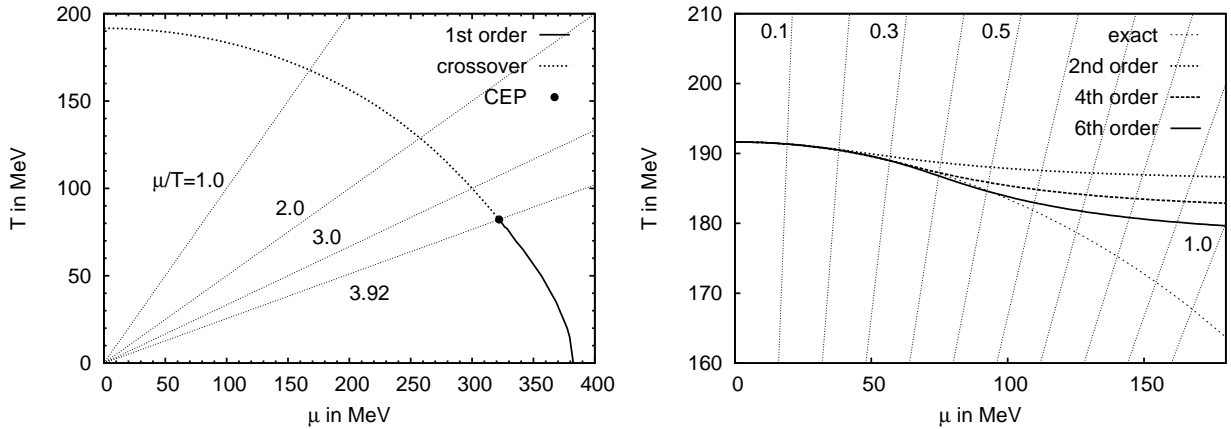


Figure 3: Phase diagram of the 2-flavor NJL model. Left: exact mean-field result for the crossover line (dotted) and the first-order phase boundary (solid). Right: comparison of the exact crossover line at small chemical potential with the reconstructed results from the Taylor expansion of the chiral susceptibility to 2nd, 4th, and 6th order. In both figures, the radial lines are lines of constant μ/T , as indicated. Adapted from Ref. [9].

However, our present focus is not on a comparison between model and lattice calculations but on a comparison within the NJL model between the “exact” phase boundary and the reconstructed result obtained from the chiral susceptibility calculated with the first few Taylor terms. This comparison is shown in the right panel of Fig. 3. As one can see, even with the 6th-order terms included, the crossover line starts to deviate from the exact result already below $\mu/T \approx 0.6$. This limit cannot be pushed much further by including more Taylor terms: As obvious from Fig. 2, higher-order Taylor terms become more and more oscillatory. As a consequence, the reconstructed chiral susceptibility does not have one, but several maxima above a certain value of μ/T and the crossover line is no longer unique.

4 The critical surface

It is now widely accepted that the finite-temperature QCD “phase transition” at $\mu = 0$ is in fact a rapid, but smooth crossover. More precisely, this is expected to be the case in the “real world” with physical masses for up, down, and strange quarks. For three massless flavors, on the other hand, the phase transition is known to be first order. Thus, if we take the nonstrange and strange quark masses as two independent variables, there is a critical line in the $m_{ud} - m_s$ plane, which separates the first-order regime at low masses from the crossover regime at higher masses (see right panel of Fig. 5). On this line, the phase transition is second order.

When we now introduce the chemical potential as a third dimension, the critical line becomes a critical surface. Until recently, it was generally expected that the critical surface is curved towards higher masses, so that the real world, which is located in the crossover regime at $\mu = 0$, may enter the first-order regime above some critical value of μ . A behavior like this is, for instance, seen in the NJL phase diagram of Fig. 3 and in many other model calculations. It is therefore often called the “standard scenario”. There are, however, indications from the lattice for a “non-standard scenario”, where the critical surface is curved towards smaller masses [11]. If this was confirmed, it would mean that the real world always stays in the crossover regime when μ is increased. This by itself does not look unusual and can be realized easily in NJL and PNJL models (see below). On the other hand, at very small quark masses, where the phase transition is first order at $\mu = 0$, the non-standard scenario would have the

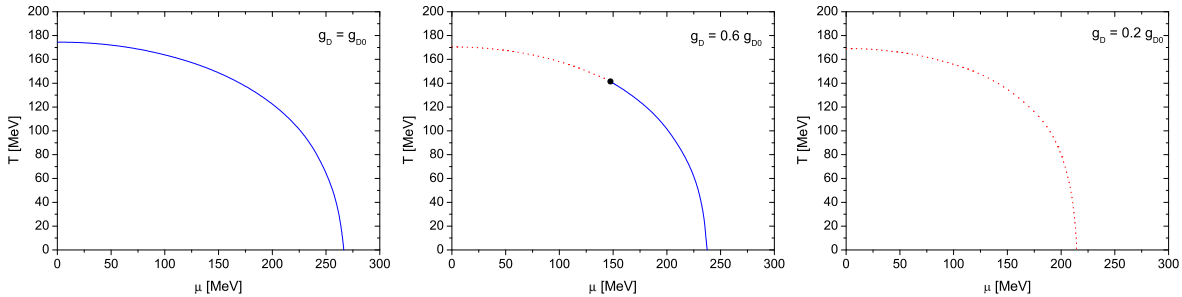


Figure 4: Phase diagrams of the 3-flavor PNJL model for unphysically small current quark masses $m_u = m_d = m_s = 0.5$ MeV and different values of the six-point coupling constant: $g_D = g_D^{(0)}$ (left), $g_D = 0.6 g_D^{(0)}$ (center), and $g_D = 0.2 g_D^{(0)}$ (right). The solid and dotted lines indicate first-order phase transitions and crossovers, respectively.

interesting consequence that there is a first-order phase transition at low values of μ which turns into a crossover above some critical value μ . Thus the question arises, whether such a “reversed” behavior is something really exotic or whether it can be realized in a simple model as well. In this context, it was recently suggested by Fukushima that the non-standard scenario could be realized within a PNJL model if a μ -dependent determinant interaction is introduced [12]. Below, we work out this idea explicitly.

Following Ref. [12] we consider a three-flavor PNJL model, given by the Lagrangian

$$\mathcal{L} = \bar{\psi}(i\not{D} - \hat{m})\psi + \mathcal{L}_4 + \mathcal{L}_6 - \mathcal{U}(\Phi, \bar{\Phi}), \quad (5)$$

where ψ is a quark field which is coupled through the covariant derivative to the Polyakov loop. The terms \mathcal{L}_4 and \mathcal{L}_6 denote local 4-point and 6-point interactions, while $\mathcal{U}(\Phi, \bar{\Phi})$ is the Polyakov loop potential. Most details of these terms are not important for the following discussion and can be found in Ref. [12]. At this point we just mention that \mathcal{L}_6 is a determinant in flavor space (“’t Hooft interaction”), which is proportional to a coupling constant g_D .

Starting with a physical parameter set [12] one finds a phase diagram which is qualitatively similar to Fig. 3, indicating that the model supports the standard scenario. In the next step we strongly decrease the current quark masses to enter into the first-order regime at $\mu = 0$. The resulting phase diagram for $m_u = m_d = m_s = 0.5$ MeV is shown in the left panel of Fig. 4. In this case, the phase transition is first order everywhere. Next, we decrease the value of the determinant coupling from the original value $g_D^{(0)}$ to smaller values. The resulting phase diagrams for $g_D = 0.6 g_D^{(0)}$ and $g_D = 0.2 g_D^{(0)}$ are shown in the two other panels of Fig. 4. Obviously, with decreasing g_D the first-order transition becomes gradually replaced by a crossover and eventually disappears completely. However, in particular the phase diagram in the center still looks “normal”, with a first-order transition at higher μ and a crossover at lower μ . Nevertheless, the series of phase diagram displayed in Fig. 4 shows that the reversed situation could be realized if we introduce a coupling which drops sufficiently fast with μ [12]. This is explicitly demonstrated in the left part of Fig. 5, where we have chosen an exponentially dropping coupling constant, $g_D(\mu) = g_D^{(0)} \exp(-\mu^2/\mu_0^2)$. The constant $\mu_0 = 168$ MeV was simply introduced by hand to see the desired effect and has no deeper meaning so far.

As argued above, the reversed form of the phase diagram shown in the left part of Fig. 5 is a hint for a non-standard critical surface. This is confirmed by the results shown in the right part of Fig. 5, where the critical lines in the $m_{ud} - m_s$ plane are shown for $\mu = 0, 100$ MeV and 200 MeV. We see that the critical surface is indeed curved towards lower masses in this case. This example demonstrates that the non-standard scenario can be realized in a relatively simple model. Moreover, since the determinant

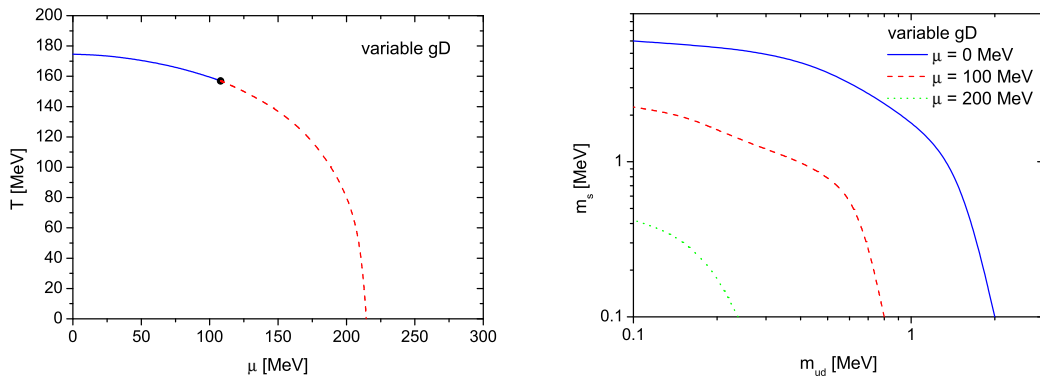


Figure 5: Left: Phase diagram of the 3-flavor PNJL model for unphysically small current quark masses $m_u = m_d = m_s = 0.5$ MeV and a μ -dependent six-point coupling constant $g_D(\mu) = g_D^{(0)} \exp(-\mu^2/\mu_0^2)$, where $\mu_0 = 168$ MeV. Right: corresponding critical lines for $\mu = 0, 100$ MeV and 200 MeV in the plane of nonstrange and strange current quark masses. The first-order (crossover) regime is to the lower left (upper right) of these lines.

interaction is related to instanton effects, which are known to decrease with increasing density, the choice of the μ -dependent g_D appears quite natural. Of course, it remains to be investigated whether our parameterization of $g_D(\mu)$ makes sense also quantitatively. Furthermore, we should introduce a T -dependence of g_D as well. In fact, this could have the opposite effect.

Acknowledgments

This talk was partially based on common work with D. Blaschke, M.K. Volkov, and J. Wambach, who we wish to thank for a fruitful collaboration. Financial support by the Heisenberg-Landau programme (M.B. and A.E.R.), by the grant of the Russian President (A.E.R.), by CONICET and EMMI (A.G.G.) and by DFG (M.B.) are gratefully acknowledged.

References

- [1] P.N. Meisinger and M.C. Ogilvie, PLB 379 (1996) 163
- [2] K. Fukushima, PLB 591 (2004) 277
- [3] C. Ratti, M.A. Thaler and W. Weise, PRD 73 (2006) 014019
- [4] D. Blaschke, M. Buballa, A.E. Radzhabov and M.K. Volkov, *Yad. Fiz.* 71 (2008) 2012
- [5] F. Karsch, E. Laermann and A. Peikert, PLB 478 (2000) 447
- [6] A. Ali Khan *et al.* [CP-PACS collaboration], PRD 64 (2001) 074510
- [7] C. Schmidt, f. RBC-Bielefeld and H. Collaborations, preprint arXiv:0810.4024 [hep-lat].
- [8] C.R. Allton *et al.*, *Phys. Rev. D* 71 (2005) 054508
- [9] D. Scheffler, *NJL model study of the QCD phase diagram using the Taylor series expansion technique* (BSc thesis, TU Darmstadt, 2007)
- [10] S. Rößner, T. Hell, C. Ratti and W. Weise, *Nucl. Phys. A* 814 (2008) 118
- [11] P. de Forcrand and O. Philipsen, *JHEP* 0701 (2007) 077
- [12] K. Fukushima, *Phys. Rev. D* 77 (2008) 114028, *Erratum-ibid. D* 78 (2008) 039902